Journal of Hydrology 562 (2018) 435–445

Contents lists available at ScienceDirect

Journal of Hydrology

journal homepage: www.elsevier.com/locate/jhydrol

Research papers

Meteoric water lines in arid Central Asia using event-based and monthly data

Shengjie Wang[a,b,c], Mingjun Zhang[a,*], Catherine E. Hughes[d], Jagoda Crawford[d], Gaofei Wang[e], Fenli Chen[a], Mingxia Du[a], Xue Qiu[a], Su'e Zhou[a]

[a] College of Geography and Environmental Science, Northwest Normal University, Lanzhou 730070, China
[b] State Key Laboratory of Cryospheric Sciences, Northwest Institute of Eco-Environment and Resources, Chinese Academy of Sciences, Lanzhou 730000, China
[c] Institute of Desert Meteorology, China Meteorological Administration, Urumqi 830002, China
[d] Australian Nuclear Science and Technology Organisation, Locked Bag 2001, Kirrawee DC, NSW 2232, Australia
[e] Meteorological Bureau of Kizilsu Kirgiz Autonomous Prefecture, Artux 845350, China

ARTICLE INFO

This manuscript was handled by A. Bardossy, Editor-in-Chief, with the assistance of Philippe Negrel, Associate Editor

Keywords:
Stable isotope
Local meteoric water line
Arid Central Asia
Precipitation-weighted regression

ABSTRACT

The local meteoric water line (LMWL) reflects the relationship between stable oxygen and hydrogen isotopes in precipitation, and is usually calculated using an ordinary least squares regression (OLSR). When event-based data are used to calculate a LMWL, the differences in precipitation amount of samples are not considered using OLSR, which in turn may influence the representativeness of the LMWL for local hydrology. Small rain events occur widely in arid Central Asia (annual mean precipitation < 150 mm), and where smaller precipitation has lower deuterium excess, this results in LMWLs with slopes and intercepts lower than the global average. Based on an observation network of isotopes in precipitation across the Tianshan Mountains in arid Central Asia, LMWLs for 23 stations are calculated from event-based data from 2012 to 2013 (n = 978), using ordinary least squares, reduced major axis and major axis regressions and their precipitation-weighted counterparts. For the northern slope and mountainous areas, the LMWL slope and intercept are close to the Global Meteoric Water Line (GMWL), but the slope and intercept are lower for the southern slope indicating the greater dominance of sub-cloud evaporation. The effect of moisture recycling in the irrigated areas on the northern slope also can be seen where the LMWL slopes are > 8. Using a precipitation weighted regression method with event-based data (especially precipitation-weighted reduced major axis regression, PWRMA) is generally consistent with the OLSR regression using monthly data. However, event-based datasets provide a wider range of values to better constrain the regression than can be achieved using monthly data over a short period, providing a sounder basis for determining LMWLs for relatively short-term sampling campaigns in an arid setting. The use of the PWRMA regression is preferred for determining the LMWL for the Tianshan Mountains, and results in a regional meteoric water line of $\delta D = 7.9\delta^{18}O + 10.16$.

1. Introduction

The stable isotopes of hydrogen (δD) and oxygen (δ^{18}O) in precipitation have been widely applied in studies of hydrological processes (e.g., Aggarwal et al., 2016; Sprenger et al., 2016; Zhang and Wang, 2016; Fischer et al., 2017), and the relationship between δD and δ^{18}O in precipitation underpins many studies using isotopic approaches. A strong linear relationship between δD and δ^{18}O in natural water was noticed in the mid-20th century (Friedman, 1953). Based on approximately 400 samples (~40% from North America and the rest distributed across the world), the best-fit line of $\delta D \sim \delta^{18}O$ ($\delta D = 8\delta^{18}O + 10$) was presented by Craig (1961), and was later named the global meteoric water line (GMWL). With the establishment of the Global Network of Isotopes in Precipitation (GNIP) (IAEA/WMO, 2017), the GMWL was updated using longer time series and more stations worldwide (e.g., Yurtsever and Gat, 1981; Rozanski et al., 1993; Gourcy et al., 2005), which confirmed that $\delta D = 8\delta^{18}O + 10$ was still a good approximation for the GMWL. The equation relating δD to δ^{18}O at a site is defined as a local meteoric water line (LMWL), and can provide a reference point for interpretation of stable isotopic compositions of a range of water samples in an area. Influenced by many geographic and meteorological factors, the slopes and intercepts of LMWLs vary depending on location. The comparison of the LMWL and GMWL can be used to assess moisture sources and precipitation processes and may

* Corresponding author.
E-mail address: mjzhang2004@163.com (M. Zhang).

https://doi.org/10.1016/j.jhydrol.2018.05.034
Received 22 January 2018; Received in revised form 4 May 2018; Accepted 12 May 2018
Available online 16 May 2018

indicate the degree of sub-cloud evaporation or the contribution of re-evaporated moisture to precipitation at a site.

An ordinary least squares regression (OLSR) is widely used to determine the LMWL, and this regression method logically gives all data points equal weighting (IAEA, 1992; Hughes and Crawford, 2012). Regarding the data used to calculate the regression, three options are commonly considered: 1) Use each month of data or each sample for event-based sampling; 2) Use the precipitation amount weighted average $\delta^{18}O$ and $\delta^{2}H$ values for each month ($n = 12$); and 3) Use annual precipitation amount weighted averages of $\delta^{18}O$ and $\delta^{2}H$ (n = years of record). To reduce the influence of precipitation amount on LMWL, monthly and annual weighted values have been recommended by the IAEA (1992). The method of pooling all samples in one month and measuring the composite (as is generally done for GNIP stations) does in fact partly weight the data for the size of events, particularly where rainfall occurs frequently.

The isotopic composition of event-based samples can provide detailed information about water processes, especially the short-term water vapor transport and rainout (e.g., Risi et al., 2008; Baldini et al., 2010; Crawford et al., 2013). During recent years, stable isotopes in event-based precipitation have been widely investigated, often based on sampling durations of approximately one or two years. The relatively short duration of studies may increase the uncertainty of LMWLs determined using event-based samples. Impacted by secondary evaporation of falling raindrops in the atmosphere, the equations relating δD to $\delta^{18}O$ for smaller amount events usually show lower slopes and intercepts (Peng et al., 2007), and light precipitation events usually have a relatively enriched $\delta^{18}O$ (Dansgaard, 1964; Bony et al., 2008) and low deuterium excess (D-excess, defined as $d = \delta D\text{-}8\delta^{18}O$) (Liu et al., 2008; Wu et al., 2015). In some studies, the smaller precipitation samples are even totally excluded in calculation (e.g., Harvey, 2001; Hughes and Crawford, 2013). Small rain events, which occur widely in arid and semi-arid regions (Fu et al., 2008; Liu et al., 2011), may therefore influence the representativeness of a LMWL for local conditions. In studies of major flow processes and water storage, heavy rainfall events normally play a dominant role, and applying equal weights to each sample may lead to a hydrologically unrepresentative result. Alternative methods (including precipitation-weighted approaches) are therefore valuable in determining LMWLs, especially in arid climates (Hughes and Crawford, 2012; Crawford et al., 2014).

Besides OLSR, a reduced major axis least squares regression (RMA) was introduced by IAEA (1992), and is suitable for the constant ratio of y and x-value standard deviations. An error-in-variables generalized least squared regression (GENLS) was presented by Argiriou and Lykoudis (2006), and allowed the errors of variables to be non-constant and instead incorporate the measurement uncertainties. Hughes and Crawford (2012) introduced the use of precipitation-weighted least squares regression (PWLSR) which can reduce the biases of small rainfall events to increase the usefulness for groundwater and surface hydrology applications. Crawford et al. (2014) then introduced two additional precipitation-weighted regressions to determine LMWL, and made a comparison between these and non-weighted regressions using GNIP data; all regressions result in a similar fit if a strong linear relationship exists, but the difference in fit is significant for some coastal and oceanic sites with a poor linear relationship between δD and $\delta^{18}O$ (even though monthly precipitation weighted values were used). In the current version of IAEA (International Atomic Energy Agency) Water Isotope System for Data Analysis (IAEA/WMO, 2017), three types of LMWL are available for each GNIP station, including OLSR, RMA and PWLSR.

The arid region of Central Asia lies at the inland of the Eurasian continent, where marine moisture from surrounding oceans rarely reaches (Fig. 1). The westerlies and polar vapor are usually considered as the dominant precipitation sources (Araguás-Araguás et al., 1998; Tian et al., 2007; Wang et al., 2017; Yao et al., 2013; Zhang and Wang, 2018). Regional mean precipitation in arid Central Asia is < 150 mm per year (Chen, 2012), ranging from < 10 mm at some desert basins to > 500 mm at some mountainous sites. The Tianshan Mountains (also known as Tien Shan), spanning multiple countries, are the main mountain ranges in arid Central Asia. A series of oases are distributed along the northern and southern slopes of the Tianshan Mountains, and many low-lying deserts such as the Taklimakan and Gurbantunggut deserts lie near the mountains. The oasis belt is also called the Tianshan Corridor, and is a vital section of the ancient Silk Road. In such an arid region, the local meteoric water line is an important reference in hydrological studies, and development of a meteoric water line using limited precipitation samples needs to be carefully considered (Oberhänsli et al., 2009; Huang and Pang, 2010). However, across the Tianshan Mountains the only existing LMWLs are for several closely located sites near Urumqi (Pang et al., 2011; Liu et al., 2014) and for the whole region (Wang et al., 2016c). In this study, LMWLs for 23 sampling stations covering ~500,000 km^2 across the Tianshan Mountains, China, are presented using multiple regressions. Although the observation period is still relatively short, the network provides a platform to understand the spatial pattern of LMWL. In addition, the differences between precipitation-weighted and unweighted regressions are considered, and meteorological controls on LMWLs are discussed.

2. Data and methods

2.1. Observation network

According to the physico-geographic regionalization of arid land in China (Chen, 2010), there are five natural areas across this region (Fig. 1 and Table 1): (1) The Junggar Basin desert area: This area generally lies at the northern slope of the Tianshan Mountains, and many small inland rivers flow to the northern desert. Due to the moisture path of westerlies, the precipitation amount for the western portion is larger than that for the eastern portion. (2) The Ili-Bayanbulak mountain area: This area generally consists of a westward river valley at the western portion (Ili) and a high-altitude basin at the eastern portion (Bayanbulak). For the Ili portion, the topography of westward valley captures plenty of westerly moisture, and leads to a relatively humid climate and a westward Ili River flowing to the Balkhash Lake; For the Bayanbulak portion, a vast wetland is located at the center, and the river flows to the southern desert. (3) The Tarim Basin desert area: This area lies at the southern slope of the Tianshan Mountains, and the climate is more arid than that in the northern slope due to the rain shadow effect of surrounding high mountains (i.e., the Tianshan Mountains and the Tibetan Plateau). The inland rivers originating from the mountains flow to the southern desert. (4) The Turpan Basin desert area: The area is a very arid basin with minimum elevation of −154 m, and lies at the southern slope of the eastern Tianshan Mountains. China's long-term meteorological record with the lowest mean precipitation amount (< 10 mm) occurs for this area. (5) The Hami Gobi desert area: This area lies at the eastern extremity of the southern slope of the Tianshan Mountains, and is at the western edge of the vast Gobi desert. In 2012, an integrated observation network of stable isotopes in precipitation was established across the Tianshan Mountains, arid Central Asia (Wang et al., 2016c). In this network, all the natural areas across the Chinese Tianshan Mountains were well covered. Considering the climate type and observation network, the neighboring Hami Gobi and Turpan Basin are combined in this study (Turpan-Hami).

Under a typical continental climate, air temperature in arid Central Asia shows a seasonal variation with warm/wet summers and cold/dry winters (Wang et al., 2016c). Generally the annual mean temperatures (Fig. 2a) of Junggar and Ili-Bayanbulak are lower than the other natural areas, although the temperature in Ili-Bayanbulak shows a wide spatial variability due to the complex topography in the mountains. In Fig. 2b, the precipitation amount in Ili-Bayanbulak is usually larger than the other areas, and the very limited precipitation is seen in Turpan-Hami.

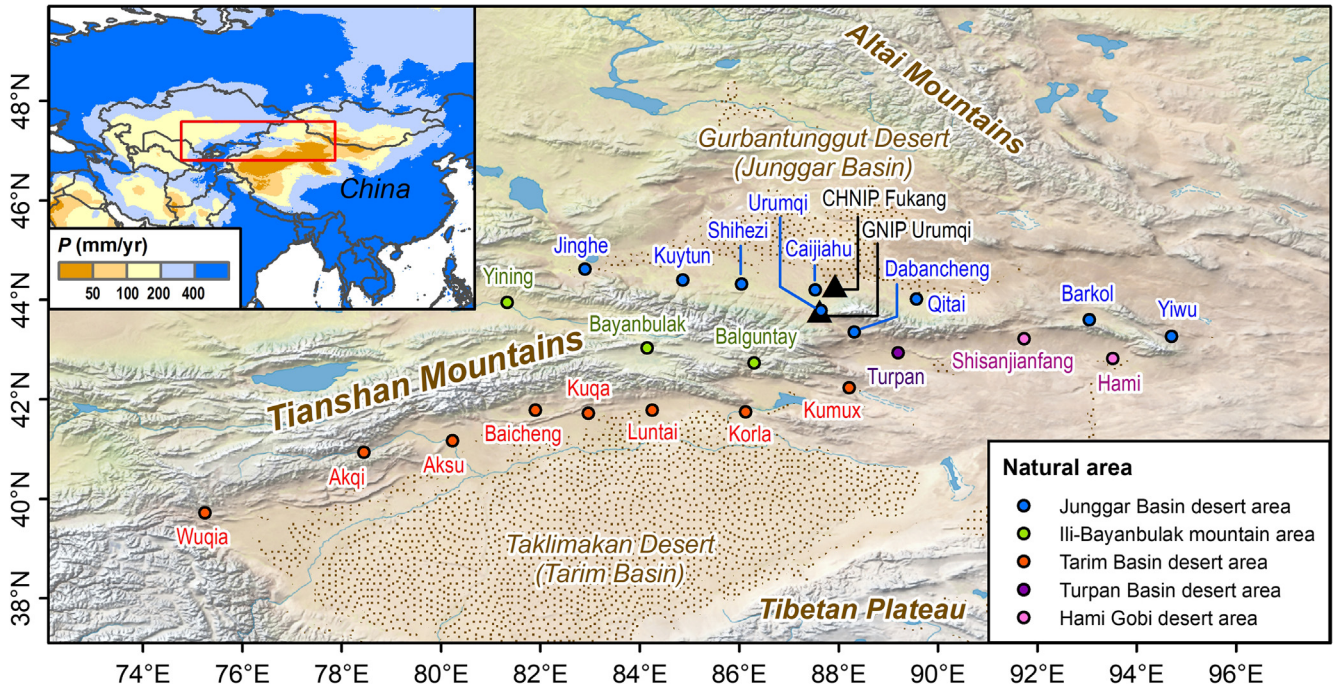

Fig. 1. Map showing the observation network of isotopes in precipitation across the Tianshan Mountains, arid Central Asia. The natural areas are based on the physico-geographic regionalization of arid land in China (Chen, 2010). Satellite-derived land cover and shaded relief were acquired from Natural Earth (http://www.naturalearthdata.com), and spatial distribution of desert is based on Wang et al. (2005). In the small map, the annual mean precipitation amount (*P*) during 1970–2000 is acquired from WorldClim-Global Climate Data (Version 2, available at http://worldclim.org; Fick and Hijmans, 2017), and the red frame denotes the Tianshan Mountains. (For interpretation of the references to colour in this figure legend, the reader is referred to the web version of this article.)

Although some sites in Tarim receive a similar magnitude of annual precipitation as Junggar, the regional mean precipitation amount in Tarim is far less than that in Junggar. Meteorological statistics during 1961–2005 (Shi et al., 2008) indicate that the annual mean precipitation at the Chinese Tianshan Mountains is 409 mm, but the amounts for the Junggar and Tarim basins are 277 mm and 66 mm, respectively. In addition, the difference between the long-term climatological averages for annual air temperature and precipitation amount and the data from this study is also shown in Fig. 2, indicating a similar temperature for the different periods, but with most sites having a higher than average precipitation during the study period. The precipitation amount during 2012–2013 is 114% of long-term average ranging from 76% to 144%

Table 1
Locations, mean meteorological parameters (*T*-air temperature, *P*-precipitation amount, and *RH*-relative humidity), and sample number (*n*) for each sampling station across the Tianshan Mountains.

Natural area	Station	Latitude	Longitude	Altitude (m)	1981–2010			Sep 2012 – Aug 2013			
					T (°C)	*P* (mm)	*RH* (%)	*T* (°C)	*P* (mm)	*RH* (%)	*n*
Junggar	Jinghe	44°37′	82°54′	320.1	8.2	112.1	62	8.4	136.1	56	37
	Kuytun	44°24′	84°52′	562.0	8.5	183.5	59	8.2	192.7	55	42
	Shihezi	44°19′	86°03′	442.9	7.8	226.9	64	7.2	231.9	62	70
	Caijiahu	44°12′	87°32′	440.5	6.5	153.8	62	6.4	189.9	58	53
	Urumqi	43°47′	87°39′	935.0	7.3	298.6	58	7.7	351.4	57	74
	Dabancheng	43°21′	88°19′	1103.5	6.9	76.7	51	7.0	92.7	50	10
	Qitai	44°01′	89°34′	793.5	5.4	200.9	61	5.4	256.1	58	39
	Barkol	43°36′	93°03′	1677.2	2.7	230.5	55	3.7	245.6	51	51
	Yiwu	43°16′	94°42′	1728.6	4.2	104.4	44	4.7	107.6	43	19
Ili-Bayanbulak	Yining	43°57′	81°20′	662.5	9.5	298.9	65	9.6	316.5	60	85
	Bayanbulak	43°02′	84°09′	2458.0	−4.2	280.5	70	−4.0	293	66	93
	Balguntay	42°44′	86°18′	1739.0	7.0	220.4	42	6.4	240.6	45	56
Tarim	Wuqia	39°43′	75°15′	2175.7	7.7	188.7	45	8.5	228	42	60
	Akqi	40°56′	78°27′	1984.9	6.8	237.7	52	7.7	343.3	45	52
	Aksu	41°10′	80°14′	1103.8	10.8	80.4	57	11.6	147.7	47	33
	Baicheng	41°47′	81°54′	1229.2	8.2	136.6	65	8.1	119.7	58	49
	Kuqa	41°43′	82°58′	1081.9	11.3	76.7	49	10.8	86.4	47	37
	Luntai	41°47′	84°15′	976.1	11.6	78.6	48	11.1	107.1	47	24
	Korla	41°45′	86°08′	931.5	12.0	59.2	46	12.7	68.6	39	22
	Kumux	42°14′	88°13′	922.4	9.8	59.9	42	8.9	77.2	46	28
Turpan-Hami	Turpan	42°56′	89°12′	34.5	15.1	15.4	39	15.4	22.2	37	20
	Shisanjianfang	43°13′	91°44′	721.4	12.5	22.6	32	12.1	6.9	32	6
	Hami	42°49′	93°31′	737.2	10.3	43.7	45	10.0	33	42	18

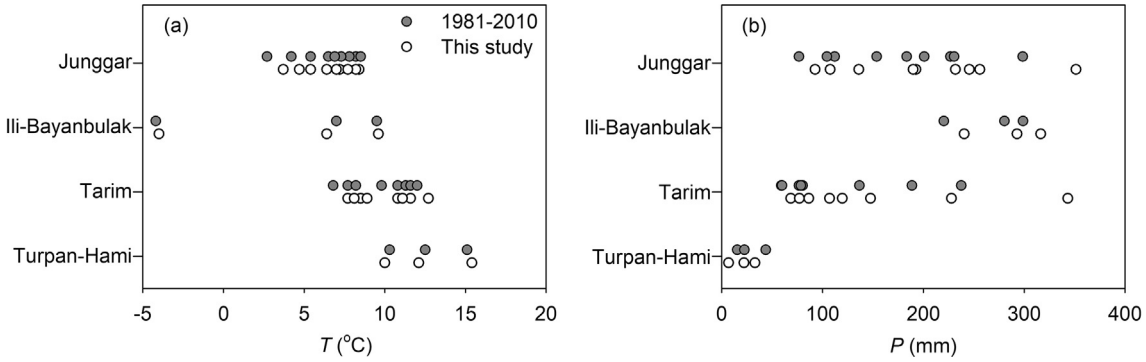

Fig. 2. Comparison of annual mean air temperature (T) and precipitation amount (P) at the sampling stations for each natural area across the Tianshan Mountains, for the long-term period (1981–2010) and this study.

except Aksu (184%) and Shisanjianfang (31%), and is 22.1 mm more than long-term average ranging between −16.9 mm and 67.3 mm except Akqi (105.6 mm). The Pearson correlation coefficients between the long-term values and those of the current study were 0.99, 0.97 and 0.95 for temperature, precipitation amount and relative humidity, respectively (with a slope of 1 for the line of best fit between long term and study period temperature and relative humidity, and 0.84 for precipitation). This indicates that the sampling period was not atypical. A more detailed comparison for each station is presented in Wang et al. (2016c).

From August 2012 to September 2013, a total of 1052 event-based precipitation samples were collected at 23 stations (Wang et al., 2016c). The basic spatial pattern of stable isotope composition in precipitation across the network was analyzed in Wang et al. (2016c), and some influencing factors including moisture recycling, below-cloud evaporation, moisture trajectory and synoptic condition were discussed in recent studies (e.g., Wang et al., 2016a,b, 2017; Zhang and Wang, 2018). In this study, a full-year subset of the samples collected from September 2012 to August 2013 was used to calculate LMWLs, and data for a total of 978 samples out of 1052 were used (representing a 12-month subset).

All the samples were collected manually as individual events by full-time meteorological observers at each station. To prevent evaporation, rain samples were collected immediately after the end of rainfall, and then stored in 60-mL HDPE (high-density polyethylene) bottles with waterproof seals. Snow samples were melted at room temperature in a plastic bag before being bottled. The precipitation amounts during the rain/snow events were measured manually. The other meteorological parameters, including air temperature and relative humidity, were recorded by automatic weather stations, and then checked against manual observations. The stable isotopic composition was analyzed using a liquid water isotope analyzer DLT-100 (Los Gatos Research, Inc.) at the Stable Isotope Laboratory, College of Geography and Environmental Science, Northwest Normal University. Every precipitation sample and isotopic standard was injected sequentially six times, and the first two injections were discarded because of memory effects. The measured results of isotopic compositions are expressed in delta notation (δ value), which is the deviation of the sample relative to the Vienna Standard Mean Ocean Water (VSMOW). The measurement precision ($\pm\sigma$) was ± 0.6‰ for δD and ± 0.2‰ for δ^{18}O, respectively. A more detailed description of sampling and analysis is found in Wang et al. (2016c).

2.2. GNIP and CHNIP data

To compare the isotopic compositions in precipitation during the sampling period and other years, the Global Network of Isotopes in Precipitation (GNIP) data from Urumqi (GNIP Site 5182801 Wulumuqi; 87°37′E, 43°47′N, 918 m a.s.l.) (IAEA/WMO, 2017) and the Chinese Network of Isotopes in Precipitation (CHNIP) data from Fukang (87°56′E, 44°17′N, 460 m a.s.l.), approximately 60 km to the north (Liu et al., 2014) were used. In the GNIP database, monthly isotopes in Urumqi precipitation were measured for 131 months, and mainly covered three periods, i.e., 1986–1992, 1995–1998 and 2001–2003. CHNIP data for Fukang are available for 48 months, 2005–2007 and 2009.

2.3. LMWL methods

Ordinary least squares regression (OLSR) is the most commonly used method in calculating a LMWL, and gives equal weighting to each sample (IAEA, 1992). Besides OLSR, reduced major axis regression (RMA) and major axis regression (MA) are two alternative regression methods without precipitation weighting (IAEA, 1992; Crawford et al., 2014). Consistent with OLSR, RMA and MA, the corresponding amount-weighted regressions defined by Hughes and Crawford (2012) and Crawford et al. (2014) are precipitation-weighted least squares regression (PWLSR), precipitation-weighted reduced major axis regression (PWRMA) and precipitation-weighted major axis regression (PWMA), respectively. All six regressions are integrated in Local Meteoric Water Line Freeware (updated in November 2014; available at http://openscience.ansto.gov.au/collection/879), and this program was applied to the samples in this study. According to Crawford et al. (2014), the average value of root mean sum of squared error ($rmSSE_{av}$) may be used to judge the regression where a value of $rmSSE_{av}$ close to 1 denotes a close fit. The s-tatistical significance is assessed using the t-test. In this study the program available at https://www.danielsoper.com/statcalc/calculator.aspx?id=103 (Soper, 2017; with method described in Cohen et al., 2003) was used to calculate the significance of the difference in slopes between two different subsets of the data, using the same regression.

3. Results and discussion

3.1. Weighted and non-weighted LMWL results

3.1.1. Spatial pattern of LMWL

Based on the 978 event-based precipitation samples collected at 23 stations across the Tianshan Mountains, meteoric water lines (MWL) were determined for each station and sub-region using the six methods outlined above (Fig. 3 and Tables S1–S3 in supplementary material). Using the most common method, OLSR, the MWL for the whole study area ($n = 978$) is $\delta D = (7.38 \pm 0.04)\delta^{18}O + (-0.33 \pm 0.55)$ ($r^2 = 0.97$, $p < 0.01$); if PWRMA is used the MWL is very close to the GMWL – $\delta D = (7.90 \pm 0.04)\delta^{18}O + (10.16 \pm 0.50)$. For individual stations, OLSR slopes range between 6.26 ± 0.33 (Luntai) and 8.30 ± 0.21 (Qitai) and are somewhat lower for the southern slope than for the northern slope and mountains. Similar patterns can also be found for the intercepts of LMWLs (Table S2).

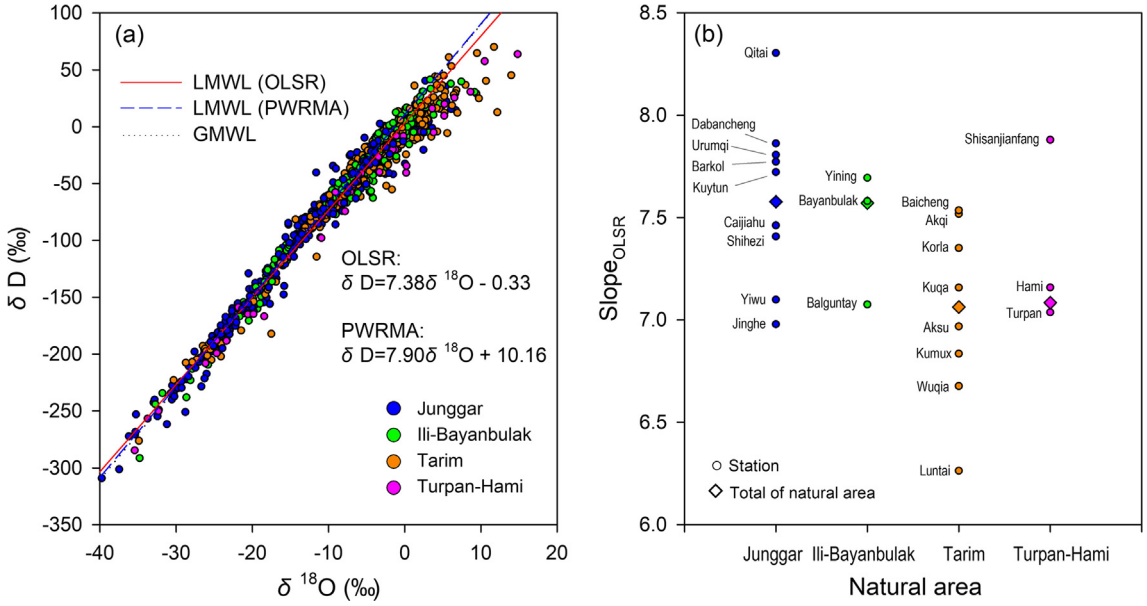

Fig. 3. (a) Correlation between δD and δ^{18}O using event-based samples across the Tianshan Mountains from September 2012 to August 2013. OLSR-based and PWRMA-based LMWLs as well as GMWL ($\delta D = 8\delta^{18}O + 10$; Craig, 1961) are shown. (b) OLSR slope using event-based data for each sampling station in the study region. The different natural areas are marked using different colors and the large diamonds represent the average of each region.

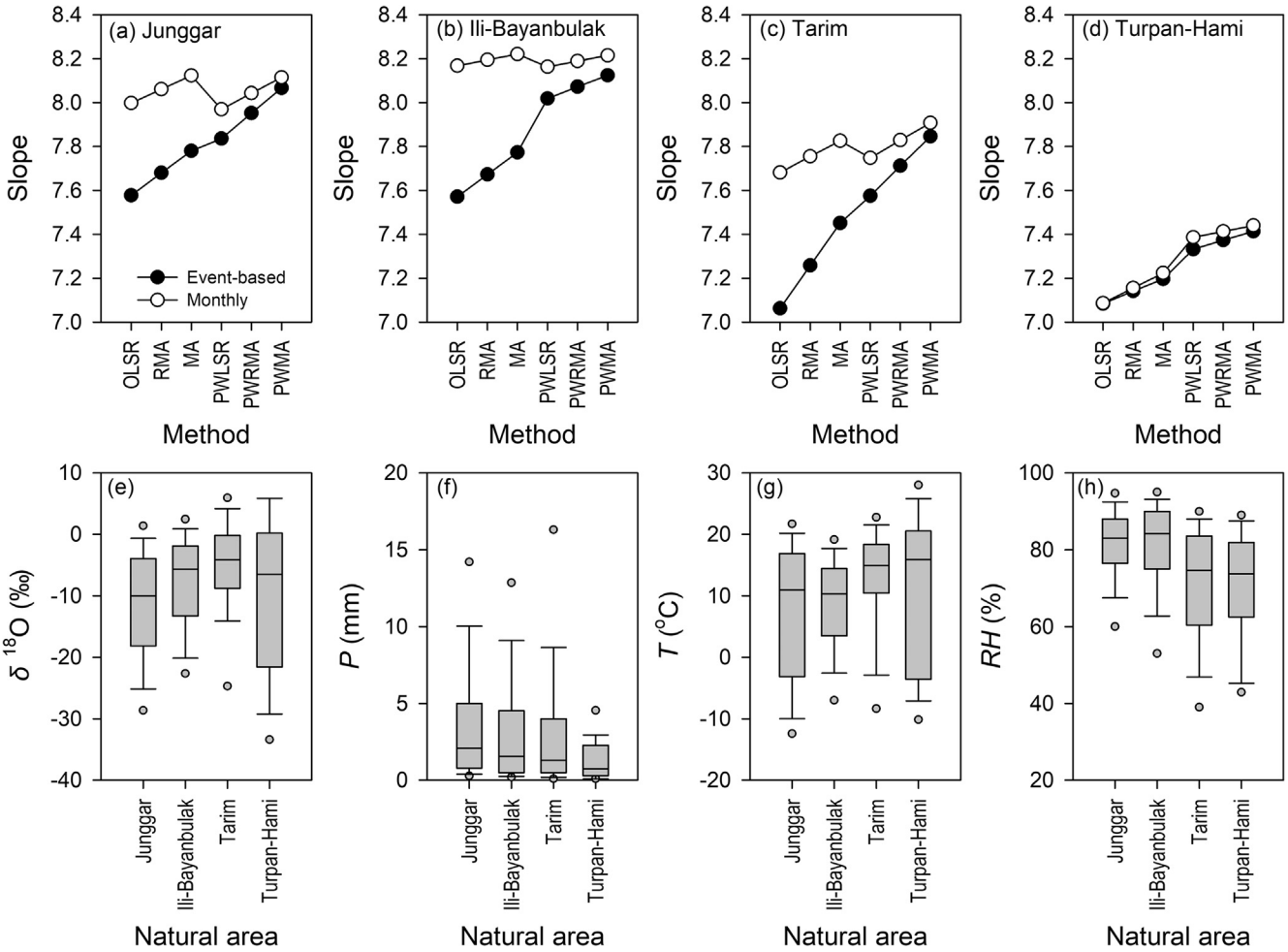

Fig. 4. LMWL slopes using event-based and monthly data (a-d), oxygen isotope ratio (e) and meteorological parameters (f: precipitation per event, g: air temperature, and h: relative humidity) for each natural area in the study region. For the box plots, the bottom of the box indicates the 25th percentile, a line within the box marks the median, and the top of the box indicates the 75th percentile; whiskers indicate the 90th and 10th percentiles; points above and below the whiskers show 95th and 5th percentiles.

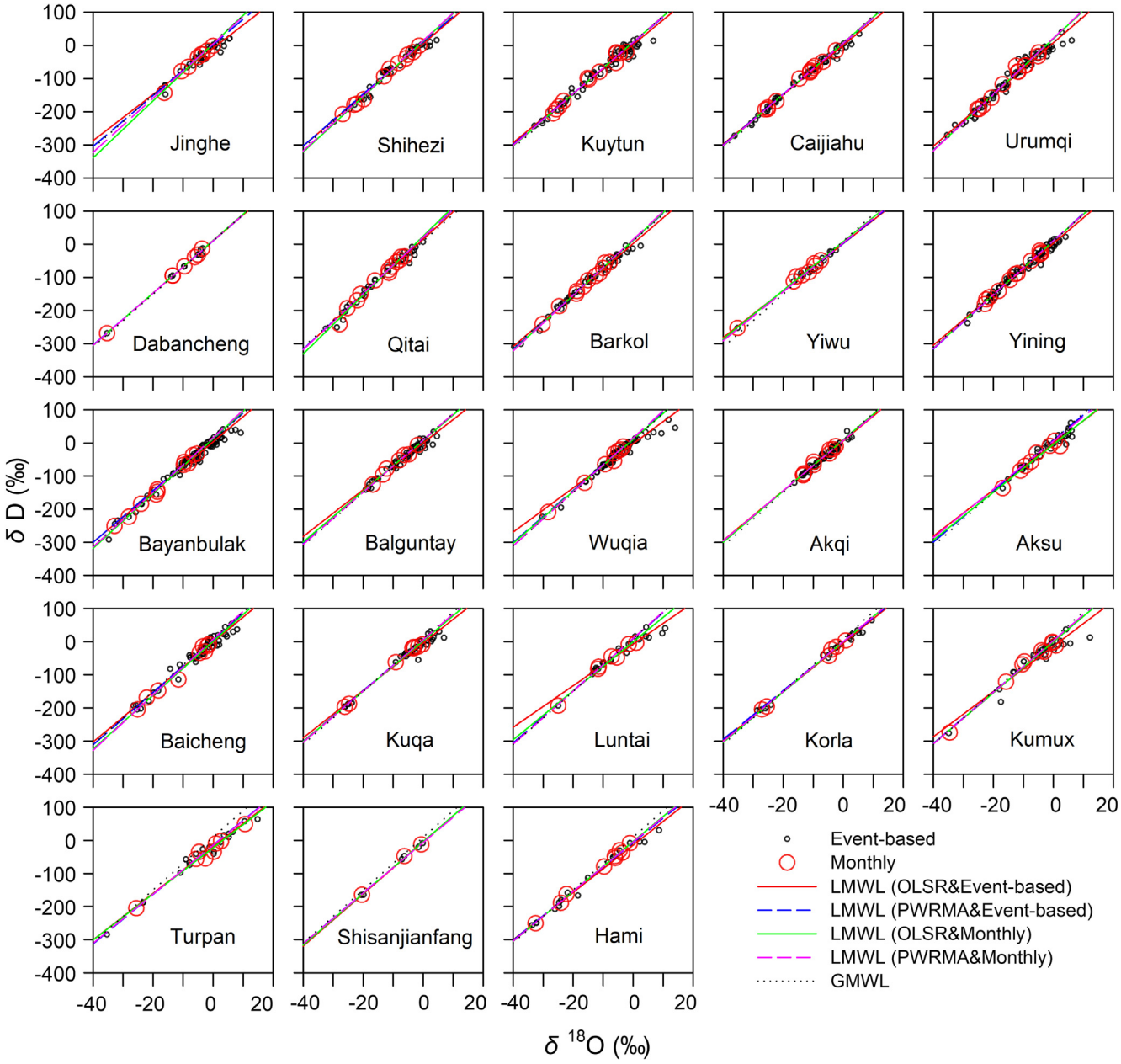

Fig. 5. Correlation between δD and δ^{18}O using event-based and amount-weighted monthly data across the Tianshan Mountains from September 2012 to August 2013.

Using the monthly precipitation weighted values from all sampling sites resulted in an OLSR meteoric water line of $\delta D = (7.67 \pm 0.08)\delta^{18}O + (3.32 \pm 1.15)$ ($n = 207$, $r^2 = 0.98$, $p < 0.01$) (Figs. 4 and 5 and Tables S4–S6 in supplementary material), where both the slope and intercept were larger than those determined using OLSR with all the event-based data. To understand the gap between event-based and monthly data, the LMWLs were calculated using alternative approaches (Figs. 4 and 5 and Tables S1–S3). In general, OLSR, RMA, MA, PWLSR, PWRMA and PWMA have an increasing trend in slope, i.e., $a_{OLSR} < a_{RMA} < a_{MA} < a_{PWLSR} < a_{PWRMA} < a_{PWMA}$ for all the samples. This order was also seen in all the natural areas. For most stations, the differences based on alternative regressions showed a trend consistent with the hypothesis that below-cloud evaporation of small rainfall amounts influences the slope of the LMWL. In most natural areas except Turpan-Hami (Fig. 4), the weighted LMWL slopes using event-based data are closer to the OLSR-based LMWL slopes using monthly data, compared with the unweighted LMWL slope. In Fig. S1, the OLSR slopes using monthly data are compared with alternative slopes using event-based data for each station. It is clear that the weighted methods using event-based samples (especially PWRMA) are generally consistent with the OLSR method using monthly data. The exception is Turpan-Hami, where using a monthly regression does not increase the slope relative to OLSR on event-based data. This is because the very low rainfall amounts in this region (Table S6) mean that even when the data is aggregated to a monthly time step a low D-excess signal can remain.

In this study, we presented LMWLs in arid Central Asia based on an observation network of 23 stations. Although the LMWL is widely used as a frame of reference in isotope hydrology, the most commonly used LMWL in this region is based on GNIP/CHNIP stations similarly located to the north of Tianshan Mountains at Urumqi and Fukang. Generally, both the OLSR slope (7.67) and intercept (3.32) in this study region are much lower than the global meteoric water line ($\delta D = 8\delta^{18}O + 10$; Craig, 1961), because of its aridity. The range of LMWLs found in this

region is not inconsistent with those found for Fukang and Urumqi by Liu et al. (2014), however the slope and intercept varies significantly over the region in a way that is not captured by previous work.

In Central Asia, the meteorological parameters (especially air temperature and precipitation amount) vary depending on location, leading to a complex spatial pattern of isotope composition and LMWL in precipitation. The study region is divided into four natural areas, and the spatial diversity in LMWL for each area reflects the different climate backgrounds. In the northern slope and the mountainous region with relatively humid conditions and low temperature, the LMWL slopes are always higher than those along the arid southern slope. Further analysis confirmed the meteorological controls on LMWL, which were consistent with the spatial pattern. The trend of LMWL with different meteorological conditions is similar to previous studies (e.g., Peng et al., 2007; Wu et al., 2015; Chen et al., 2015), and is generally presumed to be influenced by below-cloud evaporation. For the northern slope and mountainous region, the combined slope and intercept are close to the GMWL. However, along the southern slope, the LMWL slopes are lower than the GWML indicating the greater dominance of sub-cloud evaporation in this more arid sub-region, which is supported by our earlier simulation using a modified Stewart model (Wang et al., 2016b). In contrast some of the northern slope sites have a higher LMWL slope reflecting the contribution of re-evaporation from irrigated land and open water in summer (Wang et al., 2016a).

3.1.2. Meteorological controls on LMWLs

The variations in LMWLs derived using different regressions are clearly related to meteorological conditions for each station. Four meteorological parameters were considered in this study: precipitation amount (*P*), air temperature (*T*) and relative humidity (*RH*) recorded during each precipitation event. Data from all sites were combined and each of the six LMWL regressions calculated for samples corresponding to each meteorological parameter range (Fig. 6 and Tables S7–S9 in supplementary material). The linear relationship between each of these variables and the slope of the LMWL (for any method) is strong. Most precipitation events were small with 78.8% of samples (771) representing a precipitation amount ≤5 mm, and 91.7% (897 samples) being ≤10 mm. As shown in Fig. 6a, LMWLs based on lower precipitation amounts usually had lower slopes, and larger slopes were seen when using samples with larger precipitation amounts.

In Fig. 6b, the LMWL slope for events with air temperature ≥20 °C was between 5 and 7, depending on the regression method, and the slope for samples collected at < 0 °C was generally > 8. The trends in LMWL intercept (Table S8 in supplementary material) were generally similar as those of slopes. Higher slopes and intercepts were seen for the conditions of higher precipitation amount and relative humidity as well as lower air temperature. Generally, for conditions under which sub-cloud evaporation is more likely (low precipitation amounts, high temperature, low relative humidity) the slopes were smaller and a large variation was obtained using the different regression techniques.

3.1.3. Influence of heavy and small precipitation on LMWLs

The primary reason to use precipitation weighting is to ensure that heavier rainfall events influence the LMWL equation in proportion to their hydrological importance. To evaluate the importance of this across the Tianshan Mountains region, we calculated LMWLs after removing the heavy precipitation in stages ($P < 30$ mm, $P < 20$ mm and $P < 10$ mm; Table 2 and Tables S10 and S11 in supplementary material). Across the entire study region, the removal of precipitation ≥20 mm has a limited influence on LMWL slopes for any method. For the unweighted regressions the difference in slope from removing precipitation ≥10 mm was close to zero. For precipitation-weighted regressions the change in slope was also small and generally only seen clearly for the $P < 10$ mm subset.

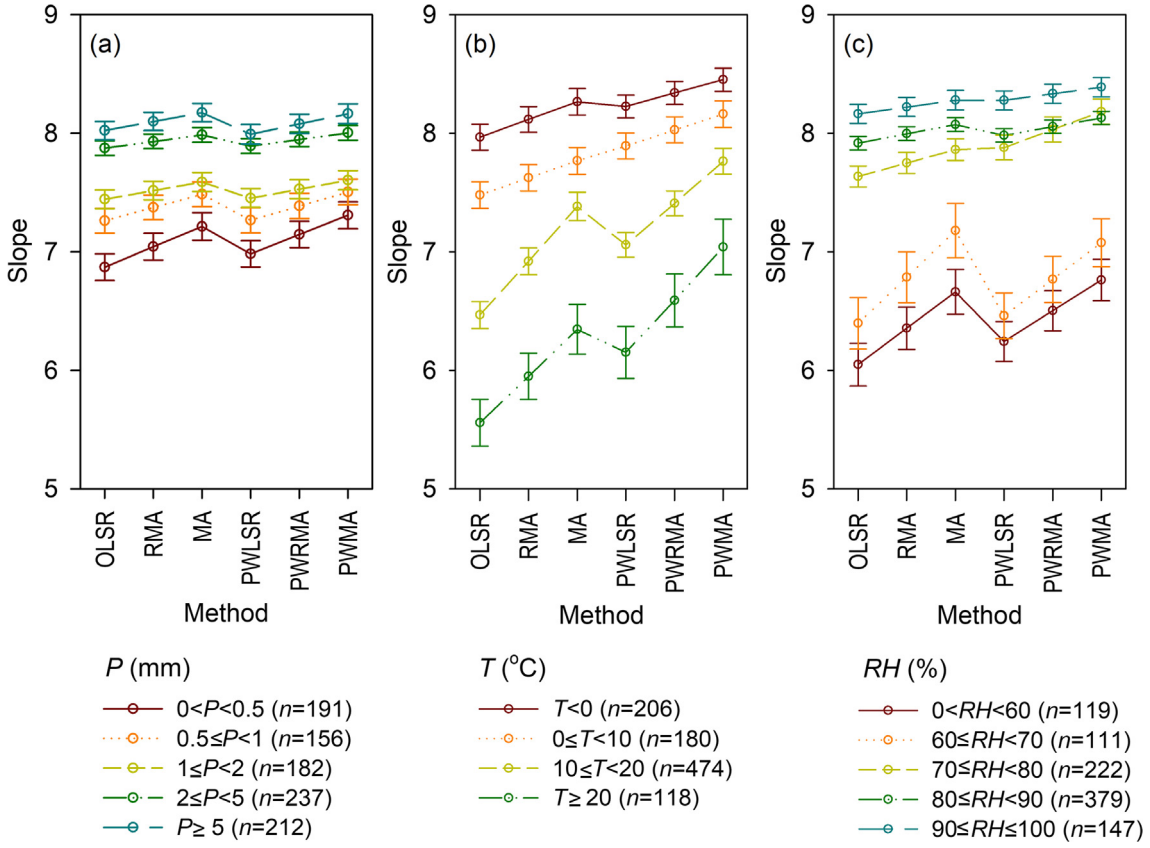

Fig. 6. LMWL slope under different meteorological conditions (*P*-precipitation amount, *T*-air temperature, and *RH*-relative humidity) using six regressions across the Tianshan Mountains from September 2012 to August 2013.

Table 2
LMWL slope ($a \pm \sigma_a$) without large and small precipitation events using six regressions across the Tianshan Mountains from September 2012 to August 2013.

P (mm)	Slope						n
	OLSR	RMA	MA	PWLSR	PWRMA	PWMA	
Total	7.38 ± 0.04	7.50 ± 0.04*	7.62 ± 0.04**	7.80 ± 0.04**	7.90 ± 0.04**	7.99 ± 0.04**	978
< 30	7.38 ± 0.04	7.50 ± 0.04*	7.62 ± 0.04**	7.80 ± 0.04**	7.89 ± 0.04**	7.98 ± 0.04**	971
< 20	7.38 ± 0.04	7.50 ± 0.04*	7.62 ± 0.04**	7.80 ± 0.04**	7.90 ± 0.04**	8.00 ± 0.04**	964
< 10	7.38 ± 0.04	7.49 ± 0.04	7.60 ± 0.04**	7.77 ± 0.04**	7.85 ± 0.04**	7.93 ± 0.04**	894
> 0.5	7.59 ± 0.04^{++}	7.68 ± 0.04^{++}	7.78 ± 0.04$^{**,++}$	7.82 ± 0.04**	7.92 ± 0.04**	8.01 ± 0.04**	809
> 1	7.72 ± 0.05^{++}	7.81 ± 0.05^{++}	7.89 ± 0.05$^{**,++}$	7.87 ± 0.05*	7.96 ± 0.05**	8.05 ± 0.05**	651
> 5	8.01 ± 0.08^{++}	8.10 ± 0.08^{++}	8.19 ± 0.08^{++}	7.99 ± 0.08^{+}	8.09 ± 0.08^{+}	8.18 ± 0.09	219

Note: *Statistically significant difference from OLSR at the 0.05 level. **Statistically significant difference from OLSR at the 0.01 level. $^{+}$Significantly different from the "total" line of the same regression type at the 0.05 level. $^{++}$Significantly different from the "total" line of the same regression type at the 0.01 level.

The influence of small precipitation events on LMWLs is also seen in Table 2. Compared with heavy precipitation, the variations of LMWLs when removing small precipitation (0.5 mm, 1 mm or 5 mm) are much larger; this is to be expected given the lower D-excess of many of these samples. Generally, the removal of small precipitation may result in a larger LMWL slope, and the difference in slope using the unweighted regressions is larger than that using the precipitation-weighted regressions; in effect the removal of small precipitation amounts may be considered an arbitrary alternative to precipitation weighting and for precipitation-weighted regressions the effect of these small rainfall events is already minimized. It is significant for many of the non-weighted regressions but hardly at all for the weighted regressions, proving that weighting really is effective at removing any bias due to sample amount. The removal of rainfall of < 1 mm or < 5 mm is equivalent to precipitation weighting for each of the regressions. The results when only those precipitation amounts of > 5 mm were used, indicate little difference in the slopes between the different regression techniques.

3.2. Necessity and potential application of weighted regressions

A key question to consider is: given the small difference statistically between weighted and non-weighted regressions, is it justified to use weighted regressions at all? Statistically one might say No. However, the effect of weighting is clearly increasing the slope in all cases and, if we agree that the justification for weighting of removing a systematic bias in the regression is sound, then this should be considered the standard rather than OLSR.

In the past several years, stable isotope compositions in precipitation on an event or synoptic scale have aroused great attention in China and other countries. In many studies, event-based data over a relatively short period is used directly to determine a LMWL and for comparison with MWLs using monthly GNIP station data. The potential influence of irregular sample frequency or short duration is not always considered because of the limited data availability. Interestingly, in this study the precipitation-weighted regressions using event-based data were similar to unweighted LMWLs using the monthly data, except in the most arid Turpan-Hami region. This indicates that the influence of sample frequency should be carefully considered. If we have only a short-term event-based precipitation isotope record spanning, for example, a year, especially in an arid climate, the weighted regression can be considered as a strong alternative. In some locations where seasonal variations in precipitation isotope composition are small, using event-based data rather than monthly averages may allow the slope of the LMWL to be better defined by increasing the range of input values to the regression. However, in the Tianshan Mountains the large seasonal range in the monthly averages (Fig. 4 in Wang et al., 2016c) helps to constrain the slope of the regression, which is why the effect of the amount weighting is less pronounced. Only in cases where the most depleted precipitation has a lower d-excess does the monthly average based OLSR result in a larger slope than the PWRMA (e.g. Qitai, Jinghe, Kuytun; Fig. 5). Conversely, as expected, where the most enriched precipitation has a low d-excess, the PWRMA results in the higher slope (e.g. Turpan, Luntai, Aksu; Fig. 5). In both extremes there is a strong case for balancing the influence of these extremes based on their amount.

Generally, we would expect that removing heavy precipitation events would reduce the LMWL slope, especially for the weighted methods. As stated in previous studies (Hughes and Crawford, 2012; Crawford et al., 2014), the primary purpose to use the weighted method is to ensure heavy precipitation events influence the LMWL in proportion to their hydrological importance. However, in this region, heavy precipitation events are infrequent, and the influence of heavy precipitation (especially ≥20 mm) is relatively limited. The precipitation extremes do exist, but the frequency is actually very low, although the frequency of occurrence has increased to some extent in recent decades (Wang et al., 2013a,b). In contrast, the influence of low precipitation events on LMWL is significant. In arid Central Asia, the rain events with amount < 5 mm play a dominant role. If we remove some small rain events, a great variability in LMWL parameters can be seen. Compared with the weighted regression using precipitation amount, the unweighted regression, especially OLSR, is more sensitive to the small precipitation events.

If an amount-weighted regression is considered for an event-based data series, which method is more robust or recommended? The $rmSSE_{av}$ statistic cannot be used to compare precipitation-weighted with non-weighted regressions, only within the weighted or non-weighted groups. Based on this statistical indicator, generally, PWLSR would be considered the most robust among the precipitation-weighted methods and RMA amongst the non-weighted methods. However, as discussed by Crawford et al. (2014), RMA based regressions are mathematically the most appropriate because of their equal weighting of both δD and δ^{18}O as independent but related variables in the regression; therefore, PWRMA should also be considered suitable. MA/PWMA regressions also meet the criteria but Crawford et al. (2014) comment that these regressions are more sensitive to outliers and may lead to an unexpectedly high slope, and therefore their use is not recommended.

3.3. Inter-annual variability of LMWLs

As shown in Fig. 7 and Wang et al. (2016c) and Liu et al. (2014), the seasonality of δ^{18}O in precipitation is seen in the Urumqi (Wulumuqi) GNIP data, Fukang CHNIP data and current observations in arid Central Asia. The seasonal variation of isotopic characteristics during our observation period is generally within the bounds of the long-term GNIP/CHNIP data; however, in autumn and winter it is consistently more depleted than the average. To have a comparison point for monthly and event-based LMWLs as well as the inter-annual variation of LMWLs, the GNIP/CHNIP data for Urumqi/Fukang were selected. To remove the influence of seasonal bias, the years with < 2 months of missing data when monthly precipitation was > 1 mm (i.e., 1986–1987, 1989–1991,

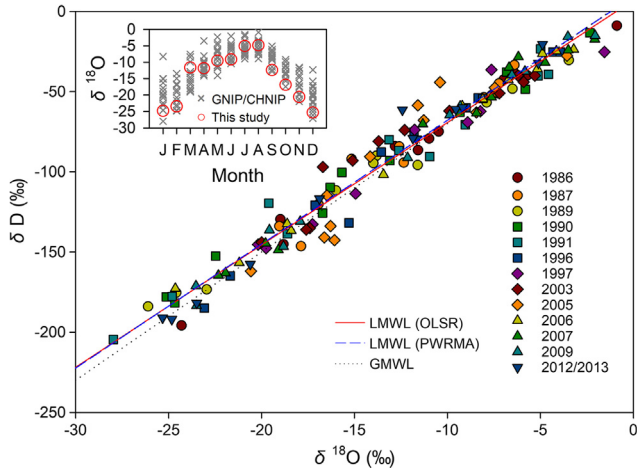

Fig. 7. OLSR-based and PWRMA-based LMWLs in Urumqi/Fukang from 1986 to 2013 (n = 147). The monthly isotopic data during 1986–2003 was provided by IAEA/WMO (2017), from 2005 to 2009 by CHNIP (Liu et al., 2014), and the event-based data during 2012–2013 were precipitation-weighted to monthly series. The small figure shows monthly variation of $\delta^{18}O$ in precipitation in Urumqi (GNIP dataset: 131 months during 1986–2003) and Fukang (CHNIP dataset: 48 months during 2005–2009) and the in-situ observations in this study.

1996–1997, 2003, 2005–2007, 2009) were used to create a LMWL for each year (Fig. 7 and Tables S12–S14 in supplementary material).

In Fig. 8 and Tables S12–S14 in supplementary material, the OLSR slope ranges between 7.06 (1991 and 2003) and 8.90 (2005), and the PWRMA slope ranges from 6.60 (2003) to 8.66 (2005). In arid Central Asia, stable isotopes in precipitation are mainly controlled by the temperature effect (Yao et al., 2013; Wang et al., 2016c). However, we observe no significant correlations between LMWL slopes derived using OLSR or PWRMA and temperature or precipitation amount at annual or seasonal time scales. The relatively larger LMWL slope in 1996 (a_{OLSR} = 8.30) and 2012/2013 (a_{OLSR} = 8.43) coincides with lower winter air temperatures in those years; this is also seen to some extent in 1986, however in 1997 which also had low winter temperature the summer temperature was very high and total rainfall amount low, and the LMWL slopes were low.

As our dataset is only for one 12-month period, we have used the GNIP station Urumqi (Wulumuqi) and the CHNIP station Fukung to consider the level of inter-annual variability. The reason for the largest LMWL slope being found at Urumqi for 2012/2013 should be considered. Is it possible that the sampling method for the GNIP station may lead to some evaporative enrichment? Huang et al. (2013) considered that possibility for data from a similar period from the Changsha GNIP station in China; they observed a large difference between the summer, but not winter, LWML slope when comparing monthly GNIP samples with their daily data. The Urumqi GNIP data has a wide range of D-excess values which show a weak negative correlation with $\delta^{18}O$, but none with precipitation amount. However, in the Urumqi GNIP dataset significantly lower D-excess was seen in summer than winter on average, whereas for this study the lower D-excess was found in winter (Wang et al., 2016c). This may be considered to support the possibility of sample evaporation in the GNIP data influencing the LMWL slope.

In addition, whilst sub-cloud evaporation may lead to a decrease in D-excess in more enriched samples, as seen throughout the region, at this site recycling of moisture from local irrigation water re-evaporated under low humidity conditions contributes to a higher D-excess during the growing season (Wang et al., 2016c). This will tend to increase the slope of the LMWL in comparison to other sites as observed in this study. As an oasis city in an arid climate, the contribution of recycled moisture to local rainfall cannot be ignored (Wang et al., 2016a; Li et al., 2016a,b; Pang et al., 2011). The recycled moisture contribution may also show a great change in the past decades because of the increasing irrigated agricultural area and urban green coverage. Irrigation water has been sourced through increasing utilization of montane runoff from the Tianshan Mountains and the completion of a scheme to bring water from the Ertix (Irtysh) River, 400 km to the north, between the GNIP data period and this study. For example, the cropland area (mostly irrigable land) in Xinjiang has enlarged from 2.8 × 10^4 km^2 in 1985 to 3.4 × 10^4 km^2 in 2000 and then to 6.1 × 10^4 km^2 in 2015, and the urban green coverage has increased from 17.3% in 1985 to 29.1% in 2000 and then to 37.9% in 2015 (Qiu, 2005; SBXUAR, 2016). Some recent meteorological studies (Hua et al., 2016; Li et al., 2018) based on reanalysis database also showed that in arid Central Asia the proportional contribution of recycled moisture has increased during past decades. For this reason, the possibility that there has been a shift in the LMWL should also be considered.

4. Concluding remarks

In this study, the spatial pattern of the local meteoric water line and its controlling factors was analyzed using an observation network in arid Central Asia. The northern slope and mountains (with relatively low temperature and higher precipitation) have LMWLs that are relatively close to the global average, and the southern slopes (with relatively high temperature and limited precipitation) have lower LMWL slope and intercept. Generally, this study has found that use of precipitation weighting is important in arid areas. LWMLs derived using a weighted regression (especially PWRMA) with event-based data are generally consistent with applying OLSR to monthly data. However, this is less true for the more arid sites, where low event numbers mean that aggregation into monthly composites does not provide effective precipitation weighting. PWRMA is considered a more mathematically sound method for determining the LMWL than PWLSR and for this reason we recommend its use in this region and other arid and semi-arid regions.

The LMWLs derived in this paper are based on a single year, and we have found that inter-annual variability of LMWL is small, but not insignificant, particularly where rainfall is scarce. In addition, changes in regional/global climate as well as changes in landuse and local water storage and recycling can result in gradual modification of LMWLs, so a presumption that LMWLs from old data represent current conditions may not be valid.

In circumstances where only short-term datasets are available, there is a benefit to be gained by using event data rather than monthly data. A precipitation weighted regression using event-based data can provide a wider range of values to constrain the regression than using a small number of monthly data point. However, the importance of capturing complete seasonal cycles still remains therefore LWML regressions should only be applied to multiples of complete 12-month periods.

Acknowledgments

The study is supported by the National Natural Science Foundation of China (No. 41771035 and 41161012), the China Desert Meteorological Science Foundation (No. Sqj2016001), the State Key Laboratory of Cryospheric Sciences (No. SKLCS-OP-2017-04) and the Northwest Normal University (No. NWNU-LKQN-15-8). The authors greatly thank the Xinjiang Meteorological Bureau and all the meteorological stations for collecting the precipitation samples and providing the meteorological records, and the colleagues in the Northwest Normal University for their help in isotopic analyzing in laboratory. We would like to acknowledge CHNIP for providing data for Fukang and the IAEA for providing GNIP data for Urumqi. We also thank Matthew Currell (RMIT University) and two anonymous reviewers for their constructive suggestions.

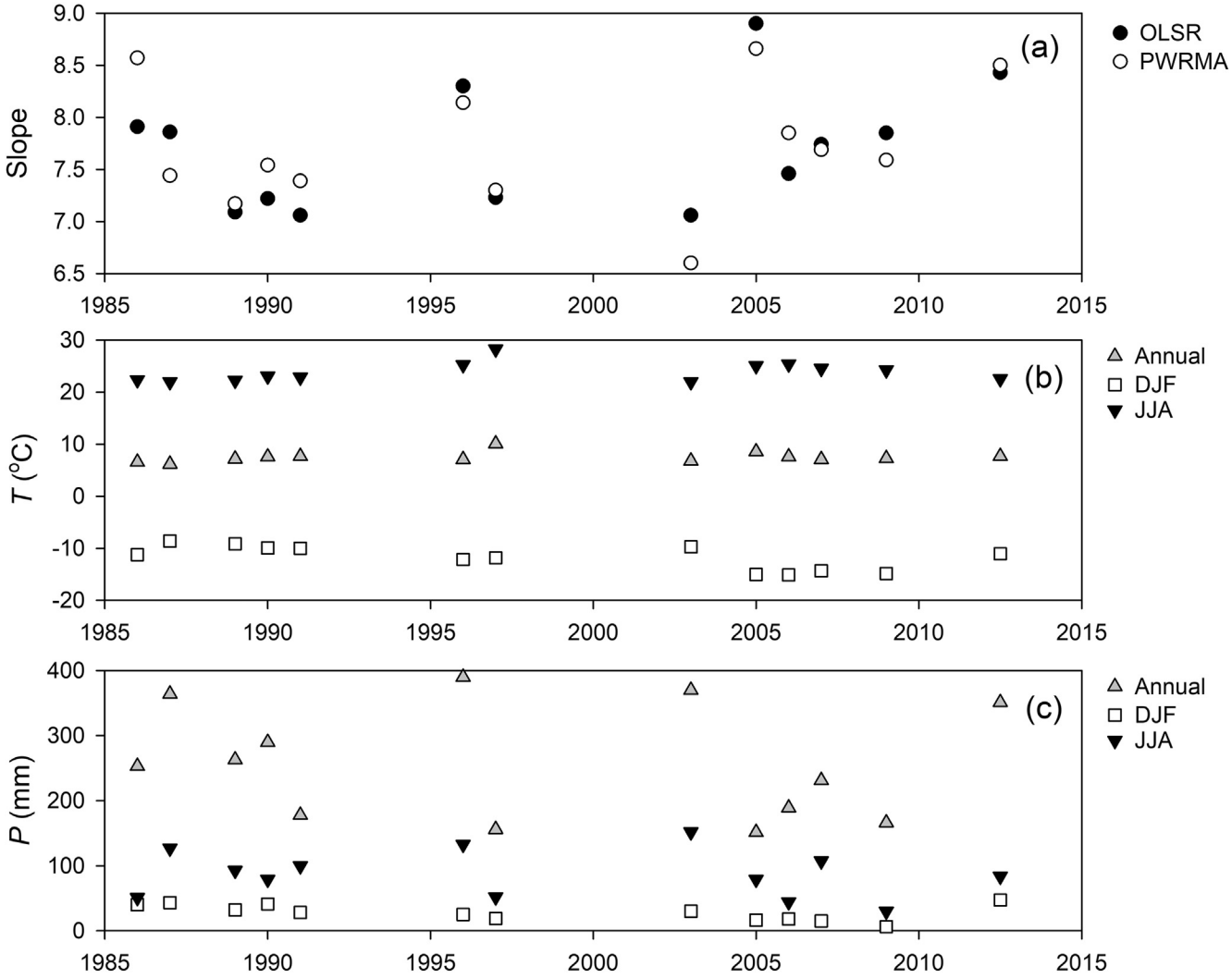

Fig. 8. Inter-annual variation of OLSR/PWRMA slope, air temperature and precipitation amount in Urumqi and Fukang from 1986 to 2013.

Appendix A. Supplementary data

Supplementary data associated with this article can be found, in the online version, at http://dx.doi.org/10.1016/j.jhydrol.2018.05.034.

References

Aggarwal, P.K., Romatschke, U., Araguas-Araguas, L., Belachew, D., Longstaffe, F.J., Berg, P., Schumacher, C., Funk, A., 2016. Proportions of convective and stratiform precipitation revealed in water isotope ratios. Nat. Geosci. 9, 624–629. http://dx.doi.org/10.1038/ngeo2739.

Araguás-Araguás, L., Froehlich, K., Rozanski, K., 1998. Stable isotope composition of precipitation over southeast Asia. J. Geophys. Res. 103, 28721–28742. http://dx.doi.org/10.1029/98JD02582.

Argiriou, A.A., Lykoudis, S., 2006. Isotopic composition of precipitation in Greece. J. Hydrol. 327, 486–495. http://dx.doi.org/10.1016/j.jhydrol.2005.11.053.

Baldini, L.M., McDermott, F., Baldini, J.U.L., Fischer, M.J., Möllhoff, M., 2010. An investigation of the controls on Irish precipitation $\delta^{18}O$ values on monthly and event timescales. Clim. Dyn. 35, 977–993. http://dx.doi.org/10.1007/s00382-010-0774-6.

Bony, S., Risi, C., Vimeux, F., 2008. Influence of convective processes on the isotopic composition ($\delta^{18}O$ and δD) of precipitation and water vapor in the tropics: 1. Radiative-convective equilibrium and Tropical Ocean-Global Atmosphere-Coupled Ocean-Atmosphere Response Experiment (TOGA-COARE) simulations. J. Geophys. Res. 113, D19305. http://dx.doi.org/10.1029/2008JD009942.

Chen, X., 2010. Physical Geography of Arid Land in China. Science Press, Beijing (in Chinese).

Chen, X., 2012. Retrieval and Analysis of Evapotranspiration in Central Areas of Asia. China Meteorological Press, Beijing (in Chinese).

Chen, F., Zhang, M., Wang, S., Ma, Q., Zhu, X., Dong, L., 2015. Relationship between subcloud secondary evaporation and stable isotope in precipitation of Lanzhou and surrounding area. Quatern. Int. 380 (381), 68–74. http://dx.doi.org/10.1016/j.quaint.2014.12.051.

Cohen, J., Cohen, P., West, S.G., Aiken, L.S., 2003. Applied Multiple Regression/Correlation Analysis for the Behavioral Sciences, 3rd edition. Lawrence Earlbaum Associates, Mahwah, USA.

Craig, H., 1961. Isotopic variations in meteoric waters. Science 133, 1702–1703. http://dx.doi.org/10.1126/science.133.3465.1702.

Crawford, J., Hughes, C.E., Parkes, S.D., 2013. Is the isotopic composition of event based precipitation driven by moisture source or synoptic scale weather in the Sydney Basin, Australia? J. Hydrol. 507, 213–226. http://dx.doi.org/10.1016/j.jhydrol.2013.10.031.

Crawford, J., Hughes, C.E., Lykoudis, S., 2014. Alternative least squares methods for determining the meteoric water line, demonstrated using GNIP data. J. Hydrol. 519, 2331–2340. http://dx.doi.org/10.1016/j.jhydrol.2014.10.033.

Dansgaard, W., 1964. Stable isotope in precipitation. Tellus 16, 436–468. http://dx.doi.org/10.1111/j.2153-3490.1964.tb00181.x.

Fick, S.E., Hijmans, R.J., 2017. WorldClim 2: new 1-km spatial resolution climate surfaces for global land areas. Int. J. Climatol. 37, 4302–4315. http://dx.doi.org/10.1002/joc.5086.

Fischer, B.M., van Meerveld, H.I., Seibert, J., 2017. Spatial variability in the isotopic composition of rainfall in a small headwater catchment and its effect on hydrograph separation. J. Hydrol. 547, 755–769. http://dx.doi.org/10.1016/j.jhydrol.2017.01.045.

Friedman, I., 1953. Deuterium content of natural water and other substances. Geochim. Cosmochim. Acta 4, 89–103. http://dx.doi.org/10.1016/0016-7037(53)90066-0.

Fu, J., Qian, W., Lin, X., Chen, D., 2008. Trends in graded precipitation in China from 1961 to 2000. Adv. Atmos. Sci. 25, 267–278. http://dx.doi.org/10.1007/s00376-008-0267-2.

Gourcy, L.L., Groening, M., Aggarwal, P.K., 2005. Stable oxygen and hydrogen isotopes in precipitation. In: Aggarwal, P.K., Gat, J.R., Froehlich, F.O. (Eds.), Isotopes in the Water Cycle. IAEA, Vienna, pp. 39–51.

Harvey, F.E., 2001. Use of NADP archive samples to determine the isotopes composition of precipitation: characterizing the meteoric input function for use in ground water studies. Ground Water 39, 380–390. http://dx.doi.org/10.1111/j.1745-6584.2001.

tb02322.x.
Hua, L., Zhong, L., Ke, Z., 2016. Precipitation recycling and soil-precipitation interaction across the arid and semi-arid regions of China. Int. J. Climatol. 36, 3708–3722. http://dx.doi.org/10.1002/joc.4586.
Huang, T., Pang, Z., 2010. Changes in groundwater induced by water diversion in the Lower Tarim River, Xinjiang Uygur, NW China: evidence from environmental isotopes and water chemistry. J. Hydrol. 387, 188–201. http://dx.doi.org/10.1016/j.jhydrol.2010.04.007.
Huang, Y., Zhang, X., Tang, F., Wu, H., Zhang, J., 2013. Variations of precipitation stable isotope and vapor origins revealed by deuterium excess in Changsha. J. Nat. Resour. 28, 1945–1954 http://dx.doi.org/10.11849/zrzyxb.2013.11.011. (in Chinese with English abstract).
Hughes, C.E., Crawford, J., 2012. A new precipitation weighted method for determining the meteoric water line for hydrological applications demonstrated using Australian and global GNIP data. J. Hydrol. 464 (465), 344–351. http://dx.doi.org/10.1016/j.jhydrol.2012.07.029.
Hughes, C.E., Crawford, J., 2013. Spatial and temporal variation in precipitation isotopes in the Sydney Basin. Australia. J. Hydrol. 489, 42–55. http://dx.doi.org/10.1016/j.jhydrol.2013.02.036.
IAEA (International Atomic Energy Agency), 1992. Statistical treatment of data on environmental isotopes in precipitation, Technical Reports Series 331. IAEA, Vienna, pp. 1–781.
IAEA/WMO (International Atomic Energy Agency/World Meteorological Organization), 2017. Global Network of Isotopes in Precipitation. https://nucleus.iaea.org/wiser.
Li, Z., Feng, Q., Wang, Q.J., Kong, Y., Cheng, A., Song, Y., Li, Y., Li, J., Guo, X., 2016a. Contributions of local terrestrial evaporation and transpiration to precipitation using $\delta^{18}O$ and D-excess as a proxy in Shiyang inland river basin in China. Global Planet. Change 146, 140–151. http://dx.doi.org/10.1016/j.gloplacha.2016.10.003.
Li, Z., Feng, Q., Wang, Q.J., Song, Y., Li, H., Li, Y., 2016b. The influence from the shrinking cryosphere and strengthening evopotranspiration on hydrologic process in a cold basin, Qilian Mountains. Global Planet. Change 144, 119–128. http://dx.doi.org/10.1016/j.gloplacha.2016.06.017.
Li, R., Wang, C., Wu, D., 2018. Changes in precipitation recycling over arid regions in the Northern Hemisphere. Theor. Appl. Climatol. http://dx.doi.org/10.1007/s00704-016-1978-4.
Liu, Z., Tian, L., Yao, T., Yu, W., 2008. Seasonal deuterium excess in Nagqu precipitation: influence of moisture transport and recycling in the middle of Tibetan Plateau. Environ. Geol. 55, 1501–1506. http://dx.doi.org/10.1007/s00254-007-1100-4.
Liu, B., Xu, M., Henderson, M., 2011. Where have all the showers gone? Regional declines in light precipitation events in China, 1960–2000. Int. J. Climatol. 31, 1177–1191. http://dx.doi.org/10.1002/joc.2144.
Liu, J., Song, X., Yuan, G., Sun, X., Yang, L., 2014. Stable isotopic compositions of precipitation in China. Tellus B 66, 22567. http://dx.doi.org/10.3402/tellusb.v66.22567.
Oberhänsli, H., Weise, S.M., Stanichny, S., 2009. Oxygen and hydrogen isotopic water characteristics of the Aral Sea, Central Asia. J. Marine Syst. 76, 310–321. http://dx.doi.org/10.1016/j.jmarsys.2008.03.019.
Pang, Z., Kong, Y., Froehlich, K., Huang, T., Yuan, L., Li, Z., Wang, F., 2011. Processes affecting isotopes in precipitation of an arid region. Tellus B 63, 352–359. http://dx.doi.org/10.1111/j.1600-0889.2011.00532.x.
Peng, H., Mayer, B., Harris, S., Krouse, H.R., 2007. The influence of below-cloud secondary effects on the stable isotope composition of hydrogen and oxygen in precipitation at Calgary, Alberta, Canada. Tellus B 59, 698–704. http://dx.doi.org/10.1111/j.1600-0889.2007.00291.x.
Qiu, Y., 2005. Fifty Years in Xinjiang: 1955–2005. China Statistics Press, Beijing (in Chinese).
Risi, C., Bony, S., Vimeux, F., Descroix, L., Ibrahim, B., Lebreton, E., Mamadou, I., Sultan, B., 2008. What controls the isotopic composition of the African monsoon precipitation? Insights from event-based precipitation collected during the 2006 AMMA field campaign. Geophys. Res. Lett. 35, L24808. http://dx.doi.org/10.1029/2008GL035920.
Rozanski, K., Araguás-Araguás, L., Gonfiantini, R., 1993. Isotopic patterns in modern global precipitation. In: Swart, P.K., Lohmann, K.C., McKenzie, J., Savin, S., Climate Change in Continental Isotopic Records. Geophysical Monograph 78, AGU, Washington, D.C., pp. 1-36.
SBXUAR (Statistic Bureau of Xinjiang Uygur Autonomous Region), 2016. Xinjiang Statistical Yearbook 2015. China Statistics Press, Beijing (in Chinese).
Shi, Y., Sun, Z., Yang, Q., 2008. Characteristics of area precipitation in Xinjiang region with its variations. J. Appl. Meteorol. Sci. 19, 326–332 (in Chinese with English abstract).
Soper, D.S., 2017. Significance of the Difference between Two Slopes Calculator. Available from http://www.danielsoper.com/statcalc.
Sprenger, M., Leistert, H., Gimbel, K., Weiler, M., 2016. Illuminating hydrological processes at the soil-vegetation-atmosphere interface with water stable isotopes. Rev. Geophys. 54, 674–704. http://dx.doi.org/10.1002/2015RG000515.
Tian, L., Yao, T., MacClune, K., White, J.W.C., Schilla, A., Vaughn, B., Vachon, R., Ichiyanagi, K., 2007. Stable isotopic variations in west China: a consideration of moisture sources. J. Geophys. Res. 112, D10112. http://dx.doi.org/10.1029/2006JD007718.
Wang, Y., Wang, J., Qi, Y., Yan, C., 2005. Dataset of desert distribution in China (1: 100,000). Cold and Arid Regions Science Data Center at Lanzhou. http://dx.doi.org/10.3972/westdc.006.2013.db.
Wang, H., Chen, Y., Xun, S., Lai, D., Fan, Y., Li, Z., 2013a. Changes in daily climate extremes in the arid area of northwestern China. Theor. Appl. Climatol. 112, 15–28. http://dx.doi.org/10.1007/s00704-012-0698-7.
Wang, S., Zhang, M., Sun, M., Wang, B., Li, X., 2013b. Changes in precipitation extremes in alpine areas of the Chinese Tianshan Mountains, central Asia, 1961–2011. Quatern. Int. 311, 97–107. http://dx.doi.org/10.1016/j.quaint.2013.07.008.
Wang, S., Zhang, M., Che, Y., Chen, F., Qiang, F., 2016a. Contribution of recycled moisture to precipitation in oases of arid central Asia: a stable isotope approach. Water Resour. Res. 52, 3246–3257. http://dx.doi.org/10.1002/2015WR018135.
Wang, S., Zhang, M., Che, Y., Zhu, X., Liu, X., 2016b. Influence of below-cloud evaporation on deuterium excess in precipitation of arid central Asia and its meteorological controls. J. Hydrometeorol. 17, 1973–1984. http://dx.doi.org/10.1175/JHM-D-15-0203.1.
Wang, S., Zhang, M., Hughes, C.E., Zhu, X., Dong, L., Ren, Z., Chen, F., 2016c. Factors controlling stable isotope composition of precipitation in arid conditions: an observation network in the Tianshan Mountains, central Asia. Tellus B 68, 26206. http://dx.doi.org/10.3402/tellusb.v68.26206.
Wang, S., Zhang, M., Crawford, J., Hughes, C.E., Du, M., Liu, X., 2017. The effect of moisture source and synoptic conditions on precipitation isotopes in arid central Asia. J. Geophys. Res. Atmos. 122, 2667–2682. http://dx.doi.org/10.1002/2015JD024626.
Wu, H., Zhang, X., Li, X., Li, J., Huang, Y., 2015. Seasonal variations of deuterium and oxygen-18 isotopes and their response to moisture source for precipitation events in the subtropical monsoon region. Hydrol. Process. 29, 90–102. http://dx.doi.org/10.1002/hyp.10132.
Yao, T., Masson-Delmotte, V., Gao, J., Yu, W., Yang, X., Risi, C., Sturm, C., Werner, M., Zhao, H., He, Y., Ren, W., Tian, L., Shi, C., Hou, S., 2013. A review of climatic controls on $\delta^{18}O$ in precipitation over the Tibetan Plateau: Observations and simulations. Rev. Geophys. 51, 525–548. http://dx.doi.org/10.1002/rog.20023.
Yurtsever, Y., Gat, J.R., 1981. Atmospheric waters. In: Gat, J.R., Gonfiantini, R. (Eds.), Stable Isotope Hydrology. IAEA, Vienna, pp. 103–142.
Zhang, M., Wang, S., 2016. A review of precipitation isotope studies in China: basic pattern and hydrological process. J. Geogr. Sci. 26, 921–938. http://dx.doi.org/10.1007/s11442-016-1307-y.
Zhang, M., Wang, S., 2018. Precipitation isotopes in the Tianshan Mountains as a key to water cycle in arid central Asia. Sci. Cold Arid Reg. 10, 27–37. http://dx.doi.org/10.3724/SP.J.1226.2018.00027.